https://doi.org/10.48048/tis.2023.5555

Modelling and Optimization of A Light Trapping Scheme in A Silicon Solar Cell Using Silicon Nitride (SiN_x) Anti-Reflective Coating

Aliah Syafiqah Zambree[1], Madhiyah Yahaya Bermakai[1,*] and Mohd Zaki Mohd Yusoff[2]

[1]Faculty of Applied Sciences, Universiti Teknologi MARA, Perlis 02600, Malaysia
[2]School of Physics and Material Studies, Faculty of Applied Sciences, Universiti Teknologi MARA, Selangor 40450, Malaysia

([*]Corresponding author's e-mail: madhiyah@uitm.edu.my)

Received: 10 August 2022, Revised: 6 September 2022, Accepted: 13 September 2022, Published: 31 May 2023

Abstract

Solar cells system has been gaining remarkable attention in the photovoltaic (PV) industry in recent years. Therefore, many people used solar cells in their life. Hence, from time to time, many industries keep improve it to get the best of efficiency of the solar cell. In this work, it presents ray tracing of light trapping (LT) schemes in thin c-Si to enhance broadband light absorption within 300 - 1,200 nm wavelength region. For the ray tracing simulation, mono c-Si wafer with 100 μm thickness is investigated and solar spectrum (AM1.5G) at normal incidence is used. Random planar and upright pyramid front surface with silicon nitride (SiN_x) anti-reflective coatings (ARC) with the difference thicknesses are the LT schemes being studies in this work. The broadband anti-reflective coating can effectively reduce the optical loss and improve the energy efficiency in the solar cells. The optical properties of the thin c-Si are analyzed with incremental LT schemes. Not only that, the current density also calculated from the absorption curve. Optical properties and current density were evaluated to find out the best thickness and refractive index of the silicon nitride (SiN_x). The initial simulation results show that the solar cell current density is about 24.81 mA/cm^2. A great J_{max} enhancement in solar cell was achieved with utilizing the ARC thickness and type of front surface. Among the 6 proposed scheme, the scheme with upright pyramid front surface of 75 nm SiN_x ARC thickness realized a good improvement in current density of 41.19 mA/cm^2. This leads to J_{max} enhancement of 66.02 % when compared to the reference c-Si.

Keywords: Photovoltaics, Solar cell, Light trapping, Ray tracing, Absorption, Silicon

Introduction

Primary energy sources take many forms, including nuclear resources, fossil fuels and renewable resources. Nuclear resources and fossil fuels such as oil, coal and natural gas are known as conventional energy that do not replenish themselves within a specific period [1,2]. However, nuclear resources and fossil fuels are limited and can cause a lot of pollution to the environment leading to adverse effects such as global warming, acid rain and soil eruption [3-5]. This results in a growing need for sustainable and clean energy sources to meet the sustainable development of human society. Solar, wind, geothermal, hydro-power and biomass are classifying as a renewable energy sources that can extensively useful to combat energy crises [6-9]. Among these renewable energy, the power of solar has gained notable attention as the clean source of renewable energy [10]. It is necessary here to clarify exactly the meaning of the word solar energy, which is known as one of the energy sources that is renewable and very useful to the environment [11,12]. It also provides electricity when it converts thermal energy to electrical energy. However, currently 12 % to well over 20 % is the range of the efficiency of the commercial silicon solar cells [13,14].

Photovoltaic technologies have been developed with the increase of solar cell studies, and there are mainly divided into 3 generations. The first generation are the traditional solar cells made of silicon materials, the second generation are those solar cells consist of thin films, such as cadmium telluride, and copper indium gallium selenide materials, whereas the third generation are those made up of new materials such as organic, quantum dot, dye-sensitized and perovskite solar cells. The focus in this study is the silicon solar cell. Generally, silicon based solar cells are more efficient and longer lasting up to 25 years than non-silicon based cells [15-17]. Due to greater efficiency and lower cost of commercial photovoltaic (PV)

modules, the installed (cumulated) PV power has expanded at a rapid rate (30 - 40 % per year) in the previous 15 years and is rapidly growing worldwide. Thus, the production has reduced the cost for the solar cell and modules to the points where solar cells account for only a small portion of the total costs, while more than the other half accounted for the electrical and other components such as installation, maintenance, insurance and financing [18]. To reduce the cost, reducing the thickness of the crystalline silicon (c-Si) will help it. The thinner c-Si wafers will compromise the light absorption in the solar cell. To avoid the less absorption, the efficiency of the light trapping (LT) must be increased by depositing the ARC on the top of the solar cell [19]. A solar cell with no light trapping characteristics may have an optical path length of one device thickness, whereas a solar cell with good light trapping features may have an optical path length of 50, demonstrating that light bounces back and forth several times within the cell [20-22]. Changing the angle at which light travels in the solar cell by having it incident on an angled surface is a common way to create light trapping [23-25]. The front surface of a solar cell can be either pyramidal or planar. These 2 are commonly used in the manufacture of solar cells. The most frequent way for increasing path length by randomizing light direction is to employ pyramid textures [26,27]. It is because the light reflected during the initial bounce always gets a second chance of entrance as it strikes the pyramid wall on the opposite side. A textured surface will reduce reflection as well as link light obliquely into the silicon, resulting in an optical path length that is greater than the physical device thickness.

ARC is the one of the most extensively used in human daily life, industry, electronics and the other fields. It helps to reduce the reflection, transmission and increase the absorption of the sunlight when it strikes through the solar cell surface. ARC is also the main or important component in the PV systems and plays a big role in turning the solar cell into an effective one. SiO_2 and TiO_2 were the materials that were usually used for the ARC [28-30], but now, silicon nitride (SiN_x) has been found as an exclusive material in this industry. The main reason is due to variable refractive index (1.9 - 2.9) that can provide the ability to tailor the coating to be used in air or in a PV module. Another reason is due to significant level of passivation of the surface [31-33]. SiN_x film has a very high transparency in the spectral range of 300 - 1,200 nm. And the optical band gap falls from 5.19 to 5.09 eV. These values are similar to the optical band gap of bulk SiN_x which is 5.00 eV [34]. The absorption of light formed when incident light is reflected off the solar cells surface, transmission and reflection are the most important parameters impacting the efficiency of a solar cell conversion system. Therefore, by coating the solar cell with ARC materials, such as a single layer of SiN_x, can improve the amount of light absorbed by the cell surface, hence resolving these issues [13]. Currently, there is insufficient work in the literature which reports on systematic investigation of LT schemes in thin c-Si (with 100 μm thickness) for application in solar cells. A further improvement and optimizing of the c-Si solar cell is crucial in renewable energy sector as it will gradually become mainstream in PV industry in about 10 years from now.

In this paper, ray tracing of LT schemes in thin c-Si solar cells (with 100 μm thickness) is investigated. Six LT schemes with difference thickness of ARC are studied; 60, 75 and 80 nm SiN_x ARC each on random planar and upright pyramid front surface. Effects of these LT schemes towards reflection, transmission and absorption of the incident light in the thin c-Si absorber are analyzed. The J_{max} is calculated from the light absorption curve to relatively estimate LT performance on each scheme. Incident light of 300 - 1,200 nm wavelength region is selected, assuming unity carrier collection in the solar cells. Then, the highest photocurrent density from the best LT scheme is compared with the Lambertian limit for c-Si solar cells with 100 μm thickness.

Materials and methods

Simulation design

Using PV Lighthouse's Wafer Ray Tracer, LT schemes in thin c-Si solar cells (with a 100 μm thickness) was examined. In this simulation, some constant parameters have been used for simplification purpose. At 0 incident angle, solar spectrum of AM1.5G is used which is normal to the surface of the solar cell [35]. The ray tracing uses a maximum of 50,000 total rays with 5,000 rays per run. The optical parameters of solar cells in wavelength region of 300 - 1,200 nm are studied (with interval of 20 nm). The following constant parameters is shown in **Table 1**. Planar c-Si (without the LT scheme) is used as reference [19].

Table 1 Constant parameter of incident light simulation.

Parameter	Value
Zenith incident angle	0 °
Minimum wavelength	300 nm
Maximum wavelength	1,200 nm
Wavelength interval	20 nm
Number of rays per run	5,000
Maximum total rays	50,000
Maximum bounces per ray	1,000
Intensity limit	0.01 %

The schematic diagram of the LT schemes is illustrated in **Figure 1**. Random planar c-Si (without LT scheme) in **Figure 1(a)** is used as a reference while **Figures 1(b)** - **1(c)** shown LT schemes with various SiN_x ARC incremental in nature on different front surface. The front metal fingers are omitted in this work. Early hypothesis state that providing additional LT schemes into the thin c-Si absorber should boost light absorption in the solar cell. Seven LT schemes was proposed in this study including reference scheme as shown in **Table 2**. Scheme Ia and Ib, a 75 nm-thick SiN_x ARC (refractive index, n = 1.99) with the front random planar and upright pyramid are incorporated with the c-Si wafer respectively. This is known as a typical ARC thickness and refractive index that used on mono c-Si solar cells in PV industry [36]. The 75 nm ARC thickness is targeted to reduce the reflection from the c-Si, particularly at 600 nm, which represents the peak of AM1.5G solar spectrum. In Scheme IIa and IIb is using similar surface as Scheme Ia and Ib with increments of 80 nm-thick SiN_x ARC (refractive index, n = 2.0) [37]. Meanwhile, the Scheme IIIa and IIIb; different thickness and refractive index which is 60 nm-thick ARC with n = 2.3. This is known as the optimal refractive index and thickness of the thin film [38].

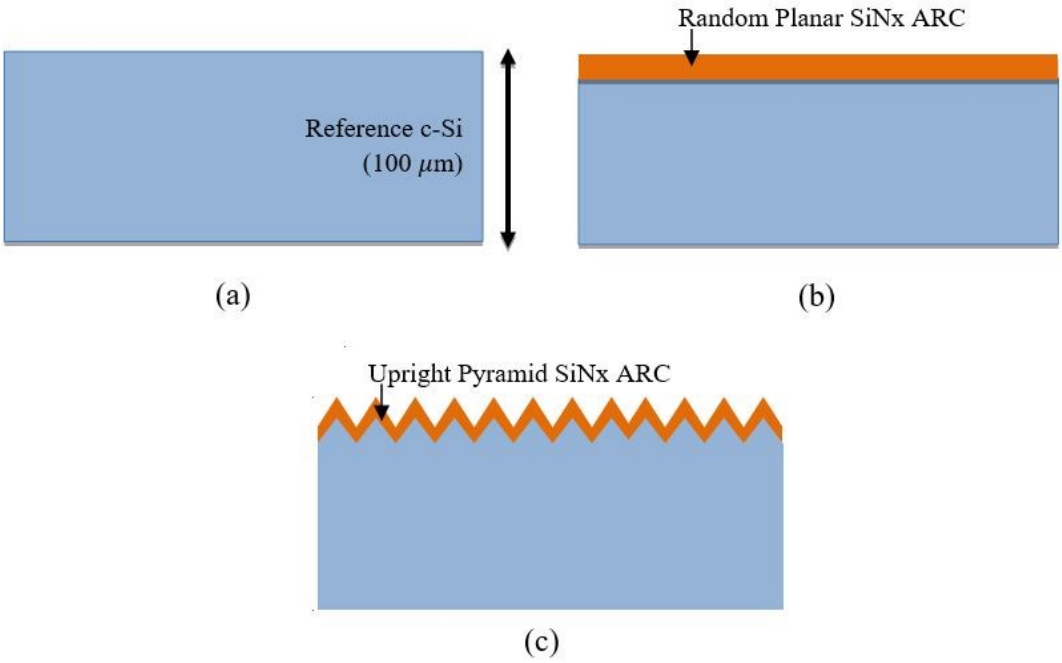

Figure 1 Schematic diagram of LT schemes in thin c-Si (with 100 μ thickness) for solar cell (a) Reference c-Si (without LT scheme), (b) Front random planar with SiN_x ARC and (c) Front upright pyramid with SiN_x ARC.

Table 2 Cross sectional simulation schemes with different thickness of ARC.

LT scheme	Thickness of Si (µm)	Thickness of SiN_x (nm)	Type of front surface	Refractive index, n
Reference scheme	100	-	-	-
Scheme Ia	100	75	Random planar	1.99
Scheme Ib	100	75	Upright pyramid	1.99
Scheme IIa	100	80	Random planar	2.00
Scheme IIb	100	80	Upright pyramid	2.00
Scheme IIIa	100	60	Random planar	2.30
Scheme IIIb	100	60	Upright pyramid	2.30

Photocurrent density (J_{max})

Total reflection, absorption, transmission in thin c-Si wafers, and J_{max} are explored and assessed using incremental LT schemes in this simulation. J_{max} is used to evaluate the LT performance of the c-Si solar cell based on the absorption data in thin c-Si. The J_{max} is determined by using the Eq. (1) to integrate the absorption curve throughout the AM1.5G solar spectrum for wavelengths 300 - 1,200 nm [39].

$$J_{max} = q \int EQE\ (\lambda).S(\lambda)\, d\lambda \quad (1)$$

where q is the electron charge and $S(\lambda)$ is the standard spectral photon density of sunlight for AM1.5G spectrum. The carrier collection in this calculation is assumed to be 1 (i.e. internal quantum, IQE = 1).

AM1.5G solar spectrum

It is necessary to consider the AM1.5G solar spectrum as shown in **Figure 2** is used to analyze the acceptability of ARC on a simulated model of solar cell. The wavelength spectrum between 300 to 1,200 nm was selected for this study. The atmospheric window opens at 300 nm wavelength and the silicon absorbed until about 1,200 nm wavelength. Radiation with a longer wavelength does not have sufficiency energy to produce electricity from a solar cell [40]. Moreover, long wavelength region which is above 900 nm will compromise the absorption of light as well as photocurrent density in the solar cell [41].

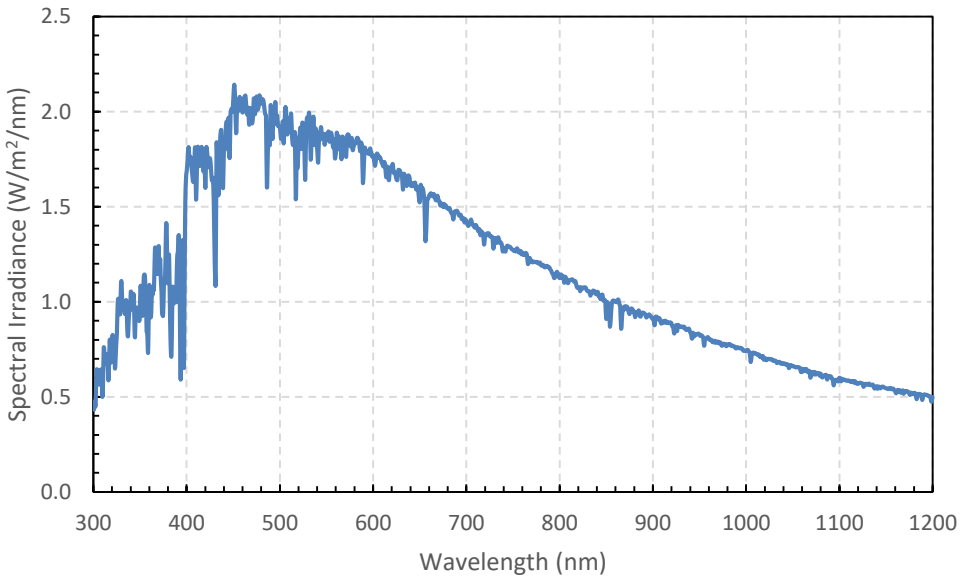

Figure 2 Solar spectrum of AM1.5G as a function of wavelength.

Results and discussion

Comparison curve of R, A and T

Figures 3(a) - 3(c) shows the reflection curves for 100 µm c-Si with incremental LT schemes on random planar and upright pyramid front surface. For comparison, the curves for the reference c-Si are presented. The graph demonstrates that the reference of c-Si has the highest reflection throughout the wavelength range of 300 - 1,200 nm. This pattern is due to a rapid shift in refractive index (n) as incident light passes through air (n = 1) and into c-Si (n = 3.5) [19].

With Scheme Ia (75 nm SiN_x ARC on front planar front surface), the reflection at range of 400 to 1,000 nm reduced further compared to the reference. The reflection around wavelength of 600 nm decrease to 0 %. This is to be expected, given that the ARC has a quarter-wavelength coating effect, which is designed to reduce broadband reflection and improve light coupling into the thin c-Si [42]. Meanwhile, the reflection of Scheme IIa which is addition of 80 nm SiN_x ARC on front planar surface, increase slightly compare to Scheme Ia at the wavelength of 400 to 500 nm but reduced slightly at range of 800 to 1200 nm. When the reference c-Si is added with 60 nm SiN_x ARC (Scheme IIIa), the reflection lowered reaches to 30 % compared with 36 % of Scheme IIa at 400 nm. Between 300 to 400 nm wavelengths, the behavior of the curve Scheme Ib with upright pyramid front surface shown the reflection is lowered about 28 %. The curve decrease to approximately 0 reflection starting on 460 to 900 nm and started to elevated at long wavelength. Other scheme with same front surface (Scheme IIb and IIIb) reveal similar response due to increasing the light scattering at the air pyramid interface. The decreasing of reflection means more light to be trapped on the solar cell and lead to more production of photocurrent in the solar cell. Hence, increasing the conversion efficiency in the LT scheme.

The transmission curve for all schemes is shown below with comparison among random planar front surface (**Figure 4(a)**) and upright pyramid front surface (**Figure 4(b)**). The transmission profile on identical front surface remains the same regardless of the thickness. But, it is obviously shown than upright pyramid front surface has significant effect in lowering the transmission of light on solar cell schemes. The value of reduction of transmission is almost 25 % compared to reference. Transmission of the short wavelength reduces to 0 due to the present of ARC. However, at long wavelength (above 900 nm) the transmission for all LT schemes are increasing, reaching 58 and 30 % at 1,100 nm for front planar and upright pyramid front surface, respectively. This is due to indirect bandgap semiconductor in Si so there is a long tail in absorption out to long wavelength resulting in higher transmittance [43]. This results agree with previous researcher [44-46].

The reference c-Si has weak broadband absorption, with approximately 66 % at 600 nm compare to other LT schemes (**Figures 5(a) - 5(b)**) which is reaching approximately 99 %. This is the main purpose to introduce efficient LT schemes in the thin c-Si solar cell [44]. On account of the increased light coupling by the ARC, light absorption in the c-Si improve across the wavelength range of 400 to 900 nm in all thickness of SiN_x ARC for both type of front surface. Broadband light absorption also increases significantly due to the increased light scattering from 300 to 600 nm compared to reference. From the optical results above, the device structure that gives the optimum result is the Scheme Ib. It is because the best achievement of highest absorption, lower reflection and transmission. This condition is known as the finest condition of the efficiency of solar cell.

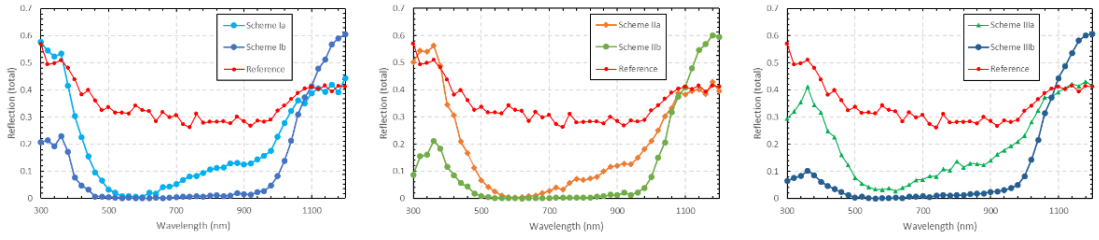

(a) (b) (c)

Figure 3 Reflection curve for thin c-Si (with 100 µm thickness) with (a) 75 nm SiN_x ARC, (b) 80 nm SiN_x ARC and (c) 60 nm SiN_x ARC. Reference c-Si included for the comparison.

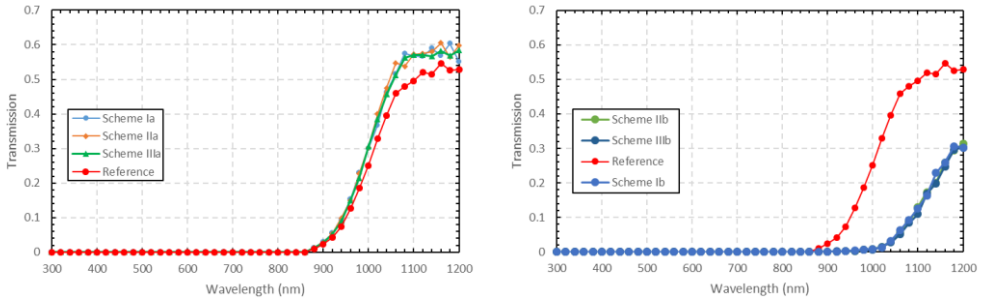

(a) (b)

Figure 4 Transmission curve for thin c-Si (with 100 µm thickness) with incremental LT schemes for (a) random planar front surface and (b) upright pyramid front surface. Reference c-Si included for the comparison.

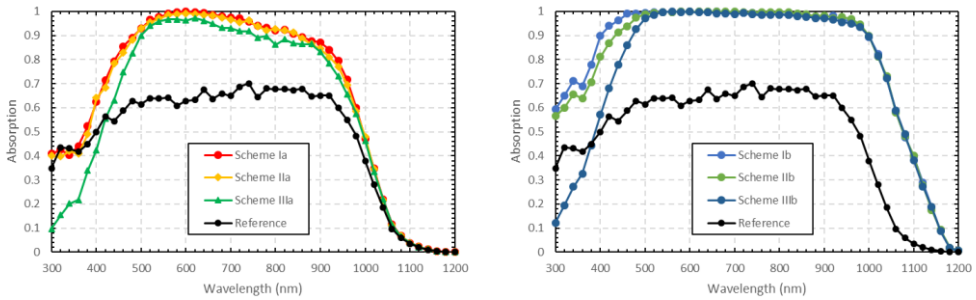

(a) (b)

Figure 5 Absorption curves for thin c-Si (with 100 µm thickness) with incremental LT schemes for (a) random planar front surface and (b) upright pyramid front surface. Reference c-Si included for the comparison.

Effect of ARC thickness on J_{max}

Table 3 summarize the calculated J_{max} of the thin c-Si (with 100 µm thickness) with incremental LT schemes. J_{max} enhancement is calculated for normalizing the J_{max} of each LT scheme to the J_{max} of the reference c-Si (without LT scheme). The reference c-Si has J_{max} of 24.81 mA/cm^2. With random planar front surface (Scheme Ia), the J_{max} increases to 35.06 mA/cm^2. This represents 41.31 % enhancement compared to the reference c-Si. This is attributed to the enhance light coupling in the 300 - 1,200 nm wavelength region into the thin c-Si by the SiN_x ARC [19]. Scheme IIa; the J_{max} increases to 34.90 mA/cm^2 or 40.67 % enhancement. Scheme III with the thickness of 60 nm of SiN_x, the J_{max} increases up to 32.98 mA/cm^2. This represents the 32.93 % enhancement compared to the reference c-Si. Meanwhile, LT schemes with upright pyramid front surface markedly increasing the J_{max} above 60 % of enhancement with Scheme Ib shown the maximum achievement by 66.02 % enhancement (41.19 mA/cm^2). This result is similar with previous finding with 40.83 mA/cm^2 [19]. This could be a guideline to fabricate a real device for utilizing in the industry. Theoretically, ARC primary function is to reduce reflected light while increasing light absorption and so improving performance of solar cell and the light is efficiently diffracted and scattered by the pyramid texture, resulting in an enhanced J_{max}. Besides, the value of J_{max} decreases as the thickness of the anti-reflection coating layer increases. The main reason is the value of refractive index between coating and the layers either side of it causes antireflective effects when utilizing a thin film. They do not require a certain thickness, but it must be thicker than a wavelength of light in order to function [47,48]. Antireflective effects from thin film coatings, on the other hand, occur when the coating is between a quarter and a half wavelength thick. This phenomenon creates destructive interference, which decreases the surface reflection. When it comes to thin films, the angle at which light reaches the surface has a greater impact on how much light is absorbed.

The simulation results are showing that the optical loss are mostly occur in external surface of the cell. **Figure 6** illustrate the optical losses caused by reflection and parasitic absorption in scheme Ib (highest J_{max}). From these curves, it is obviously shown that the best absorption in silicon solar cell take place between 500 up to 800 nm where the absorption in the front SiN_x is minimized. The absorption loss in shorter wavelengths account for almost 43 % of the total absorption. For longer wavelengths, the optical

loss in the front surface increases due to the free carrier absorption [49]. Lowering the parasitic absorption is shown to be as important as optimization of the LT scheme in increasing photocurrent density in silicon solar cell. Therefore, more attention is needed in designing the front surface of silicon solar cell in order to minimize optical losses. Nevertheless, SiNx is one of the dominated material for distinct properties such as a wide bandgap semiconductor, high radiation resistance, stability at high temperature and high thermal conductivity [50,51]. Other advantage of SiN_x is that both the elements of nitride and silicon are very abundant and non-toxic [52]. Yet, multiple approaches must be considered to acquire the optimum thickness of SiN_x ARC.

Table 3 Summary of J_{max} of thin c-Si (with 100 µm thickness) with incremental LT schemes. J_{max} of reference c-Si is included for comparison.

LT scheme	J_{max} (mA/cm^2)	J_{max} enhancement (%)
Reference c-Si (thickness = 100 µm)	24.81	-
Scheme Ia: Front random planar with 75 nm SiN_x ARC (n = 1.99)	35.06	41.31
Scheme Ib: Front upright pyramid with 75 nm SiN_x ARC (n = 1.99)	41.19	66.02
Scheme IIa: Front random planar with 80 nm SiN_x ARC (n = 2.00)	34.90	40.67
Scheme IIb: Front upright pyramid with 80 nm SiN_x ARC (n = 2.00)	40.95	65.05
Scheme IIIa: Front random planar with 60 nm SiN_x ARC (n = 2.30)	32.98	32.93
Scheme IIIb: Front upright pyramid with 60 nm SiN_x ARC (n = 2.30)	39.77	60.30

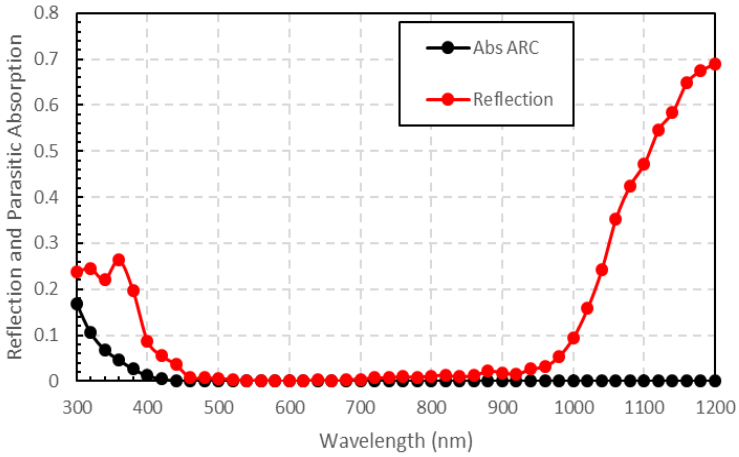

Figure 6 The curve of optical losses contribute by reflection and parasitic absorption in Scheme Ib.

External quantum efficiency (EQE)

External quantum efficiency (EQE) in silicon solar cell is the total number of electrons leaving the cell divided by the total sum of incident photons at every wavelength. The analysis of EQE is extremely important for examining the influence of the ARC on the complete performance of silicon solar cells [53-55]. Low EQE can attribute to several optical and electrical loss mechanism for charge carries in solar cell. The graph of EQE and integrated J_{max} for scheme Ib is plotted as in **Figure 7**. The EQE curve shows that the SiN_x layer can effectively improve the J_{max} of the solar cell. Result from scheme Ib shown an increasing of EQE from 65.05 to 100 % was observed in wavelength spectrum of 400 to 600 nm. The EQE curve begin to decrease starting at 700 nm to 0.03 % at 1,200 nm. This is because the light with a higher wavelength reflects less in single layer anti-reflective coating [56,57]. However, it would not significantly affect the performance of the cell. The integrated J_{max} curve keep increase in positive value at 400 to 1,100 nm and later the slope is remains constant at value of 35.06 mA/cm^2. As discussed before, high reflection and high parasitic absorption contribute the loss in J_{max} in short wavelength ranging from 300 to 400 nm.

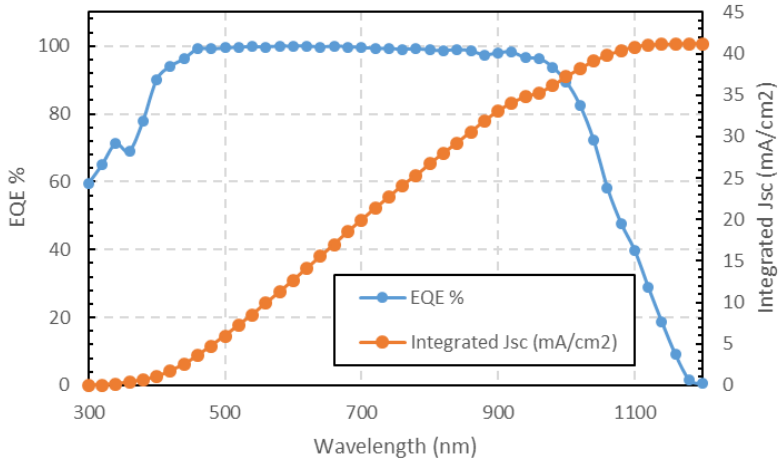

Figure 7 Percentage of EQE and integrated Jsc in upright pyramid 75 nm SiN_x ARC (Scheme Ib).

Lambertian limit

Figure 8 illustrates absorption of the substrate for Scheme Ib with J_{max} of 41.19 mA/cm^2, which represents the highest potential photocurrent density achieved in this work. Total reflection of Scheme Ib is also shown in the figure. The curve of Lambertian limit represents the highest achievable photocurrent density (J_{max}) by a solar cell with a specified device thickness [58] is also shown in the figure for comparison. Zero front reflection (R = 0) and unity rear reflection (R = 1) in solar cell geometry is the assumption used in the Lambertian limit. For the 100 µm-thick c-Si solar cell, the Lambertian J_{max} value is 43 mA/cm^2. The difference between the J_{max} of Lambertian limit and J_{max} of Scheme Ib is 1.81 mA/cm^2. The curve for absorption and reflection is opposing to each other. Highest absorption in c-Si is occur around 500 to 600 nm where lowest reflection is approximately 0.02 %. At this range the absorption curve reach the Lambertian limit. Absorption begins to decrease beyond rapidly near Infra-Red region as more light mostly transmitted through the c-Si. The optical losses caused by reflection in the short and long wavelength region is attributed to the difference stated. To reduce the optical losses in solar cell, further optimizations via ray tracing are required.

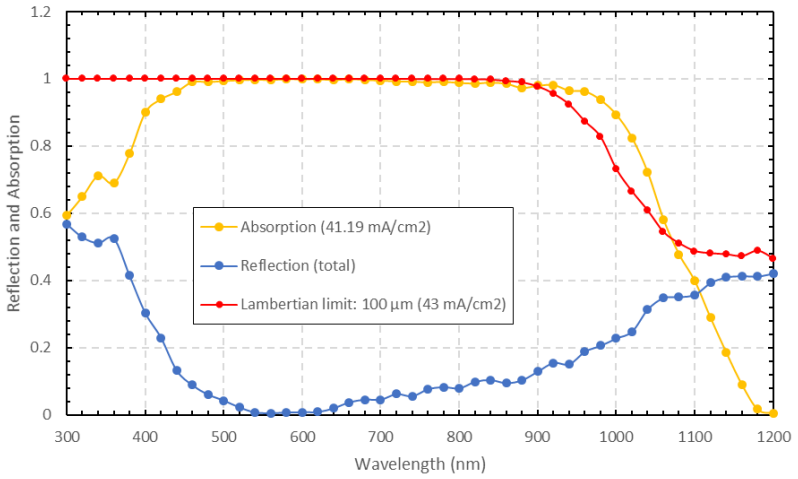

Figure 8 Reflection and absorption curve for Scheme Ib. Lambiertan limit for 100 µm-thick c-Si solar cell is used for comparison.

Conclusions

In summary, the optical behaviors on different thickness of LT layer was investigated. The reflection, transmission and absorption in the wavelength range of 300 - 1,200 nm using 6 LT schemes have been studied. The J_{max} is determine from the light absorption curve to relatively estimate LT performance on each scheme. Scheme Ib; upright pyramid front surface 75 nm SiN_x ARC with suitable match of refractive index can significantly reduce the reflectivity for short wavelength and consequently contributes towards higher short-circuit current densities J_{max} of the cell. When compared to the reference c-Si (which has a J_{max} of 24.81 mA/cm^2) the J_{max} jumps to 41.19 mA/cm^2, a 66.02 % increment. The decreasing in absorbance of light in LT scheme with random planar front surface is observed due to absence of light scattering by the ARC. The discrepancy in J_{max} between the Scheme Ib J_{max} and the Lambertian limit for the 100 µm-thick c-Si is 1.18 mA/cm^2. The optical losses in thin c-Si, which are contributed to the difference mentioned by reflection in the short and long wavelength areas. Refractive index of ARC also plays an important role in solar cell performance as it need suitable value for certain wavelength and thickness. Capturing of incident light is an essential requirement for high performance Si solar cell. The study found that the LT performance of upright pyramid is significantly better in capturing the incident light to increase the production of current density than random planar. To advance the evaluation and improvement for industrial purposes, the scheme should be developed as a real model.

Acknowledgements

Authors would like to thanks Faculty of Applied Sciences, Universiti Teknologi MARA (UiTM), Perlis Branch, Malaysia for supporting this research.

References

[1] M Kamran and MR Fazal. *Renewable energy conversion systems: Fundamental of renewable energy systems*. Academic Press, London, 2021.
[2] ASM Al-Obaidi and T NguyenHuynh. Renewable vs. conventional energy: Which wins the race to sustainable development? *IOP Conf. Ser. Mater. Sci. Eng.* 2018; **434**, 012310.
[3] P He, F Wen, G Ledwich and Y Xue. Small signal stability analysis of power systems with penetration of wind power. *J. Mod. Power Syst. Clean Energ.* 2013; **1**, 237-44.
[4] H Lala and S Karmakar. Continuous wavelet transform and artificial neural network based fault diagnosis in 52 bus hybrid distributed generation system. *In*: Proceedimgs of the IEEE Students Conference on Engineering and Systems (SCES), Allahabad, India. 2015.
[5] M Hossain and N Fara. Integration of wind into running vehicles to meet its total energy demand. *Energ. Ecol. Environ.* 2017; **2**, 35-48.
[6] A Raheem, SA Abbasi, A Memon, SR Samo, YH Taufiq-Yap, MK Danquah and R Harun. Renewable energy deployment to combat energy crisis in Pakistan. *Energ. Sustain. Soc.* 2016; **6**, 16.
[7] A Ashfaq and A Ianakiev. Features of fully integrated renewable energy atlas for Pakistan; wind solar and cooling. *Renew. Sustain. Energ. Rev.* 2018; **97**, 14-27.
[8] NA Ludin, NI Mustafa, MM Hanafiah, MA Ibrahim, MAM Teridi, S Sepeai, A Zaharim and K Sopian. Prospects of life cycle assessment of renewable energy from solar photovoltaic technologies: A review. *Renew. Sustain. Energ. Rev.* 2018; **96**, 11-28.
[9] PA Owusu and S Asumadu-Sarkodie. A review of renewable energy sources, sustainability issues and climate change mitigation. *Cogent Eng.* 2016; **3**, 1167990.
[10] GV Fracastoro. The role of renewables in the energy crisis. *E3S Web Conf.* 2014; **2**, 02003.
[11] MV Dambhare, B Butey and SV Moharil. Solar photovoltaic technology: A review of different types of solar cells and its future trends. *J. Phys. Conf. Ser.* 2021; **1913**, 012053.
[12] A Qazi, F Hussain, NABD Rahim, G Hardaker, D Alghazzawi, K Shaban and K Haruna. Towards sustainable energy: A systematic review of renewable energy sources, technologies and public opinions. *IEEE Access* 2019; **7**, 63837-51.
[13] RI Jabbar. Modeling and analysis of different anti-reflection polymer coating on silicon solar cell using PC1D software. *J. Mech. Eng. Res. Dev.* 2020; **43**, 222-32.
[14] R Swanson. A vision for crystalline silicon photovoltaics. *Progr. Photovoltaics Res. Appl*. 2006; **14**, 443-53.
[15] M Gul, Y Kotak and T Muneer. Review on recent trend of solar photovoltaic technology. *Energ. Explor. Exploit.* 2016; **34**, 4885-526.

[16] A Blakers, N Zin, KR McIntosh and K Fong. High efficiency silicon solar cells. *Energ. Procedia* 2013, **33**, 1-10.
[17] NKA Hamed, MK Ahmad, NST Urus, F Mohamad, N Nafarizal, N Ahmad, CF Soon, AS Ameruddin, AB Faridah, M Shimomura and K Murakami. Performance comparison between silicon solar panel and dye-sensitized solar panel in Malaysia. *AIP Conf. Proc.* 2017; **1883**, 020029.
[18] LC Andreani, A Bozzola, P Kowalczewski, M Liscidini and L Redorici. Silicon solar cells: Toward the efficiency limits. *Adv. Phys.* 2019; **4**, 15483053.
[19] MZ Pakhuruddin. Ray tracing of light trapping schemes in thin crystalline silison for photovoltaics. *Solid State Phenom*. 2020; **301**, 183-91.
[20] B Dale and HG Rudenberg. High efficiency silicon solar cells. *In*: Proceedings of the 14th Annual Power Sources Conference, U.S. Army Signal Research and Development Lab, New Jersey. 1960.
[21] P Campbell and MA Green. High performance light trapping textures for monocrystalline silicon solar cells. *Sol. Energ. Mater. Sol. Cell*. 2001; **65**, 369-75.
[22] SC Baker-Finch, KR McIntosh and ML Terry. Isotextured silicon solar cell analysis and modeling 1: Optics. *IEEE J. Photovoltaics* 2012; **2**, 457-64.
[23] O Hohn, N Tucher, A Richter, M Hermle and B Blasi. Light scattering at random pyramid textures: Effects beyond geometric optics. *AIP Conf. Proc.* 2018; **1999**, 030002.
[24] M Sun and PG Kik. Light trapping transparent electrodes with a wide-angle response. *Optic. Express* 2021; **29**, 24989-99.
[25] AS Blazev. *Solar technologies for 21st century*. River Publisher, Gistrup, Denmark, 2020.
[26] R Saive. Light trapping in thin silicon solar cells: A review on fundamentals and technologies. *Progr. Photovoltaics Res. Appl.* 2021; **29**, 1125-37.
[27] H Heidarzadeh, M Dolatyari, G Rostami and A Rostami. *Modeling of solar cell efficiency improvement using pyramid grating in single junction silicon solar cell. In*: A Oral, ZB Oral and M Ozer (Eds.). 2nd ed. International congress on energy efficiency and energy related materials. Springer, Cham, Switzerland, 2015.
[28] A El Amrani, I Menous, L Mahiou, R Tadjine, A Tousti and A Lefgoum. Silicon nitride film for solar cells. *Renew. Energ*. 2008; **33**, 2289-93.
[29] S Kermadi, N Agoudjil, S Samira, R Tala-Ighil and M Boumaour. Sol-gel systhesis of SiO_2-TiO_2 film as antireflection coating on silicon for photovoltaic application. *Mater. Sci. Forum* 2009; **609**, 221-4.
[30] K Ali, SA Khan and MZM Jafri. Effect of double layer (SiO_2/TiO_2) anti-reflective coating on silicon solar cells. *Int. J. Electrochem. Sci.* 2014; **9**, 7865-74.
[31] B Dieng, M Beye and AS Maiga. Optimization of silicon nitride antireflective nanostructures for silicon solar cells. *In*: Proceedings of the 7th International Energy and Sustainability Conference (IESC), Cologne, Germany. 2018.
[32] S Duttagupta, F Ma, B Hoex, T Mueller and AG Aberle. Optimised antireflection coatings using silicon nitride on textured silicon surfaces based on measurements and multidimensional modelling. *Energ. Procedia* 2012; **15**, 78-83.
[33] Y Lee, D Gong, N Balaji, YJ Lee and J Yi. Stability of SiN_x/SiN_x double stack antireflection coating for single crystalline silicon solar cells. *Nanoscale Res. Lett.* 2012; **7**, 50.
[34] N Manavizadeh, A Khodayari and E Asl-Soleimani. *An investigation of the properties of silicon nitride (SiN_x) thin films prepared by RF sputtering for application in solar cell technology*. *In*: DY Goswami and Y Zhao (Eds.). Proceedings of the ISES World Congress 2007 (Vol. I - Vol. V). Springer, Berlin, Germany, 2008, p. 1120-2.
[35] MK Ray, S Sasmal and S Maity. Optimization of multijunction solar cell by wafer ray tracer for development of high photogenerated current. *Int. J. Res. Eng. Tech.* 2015; **4**, 365-71.
[36] KWA Chee, Z Tang, H Lü and F Huang. Anti-reflective structures for photovoltaics: Numerical and experimental design. *Energ. Rep.* 2018; **4**, 266-73.
[37] C Zhou, T Li, Y Song, S Zhou, W Wang, L Zhao, H Li, Y Tang, H Diao, Z Gao, Y Duan and Y Li. SiO_x(C)/SiN_x dual-layer anti-reflectance film coating for improved cell efficiency. *Sol. Energ.* 2011; **85**, 3057-63.
[38] TW Kuo, NF Wang, YZ Tsai, PK Hung and MP Houng. Broadband triple-layer SiO_x/SiO_xN_y/SiN_x antireflective coatings in textured crystalline silison solar cells. *Mater. Sci. Semicond. Process*. 2014; **25**, 211-8.
[39] MZ Pakhuruddin, J Huang, J Dore and S Varlamov. Enhance absorption in laser-crystallized silicon thin films on textured glass. *IEEE J. Photovoltaics* 2016; **6**, 159-65.

[40] NI Ibrahim and MMBE Omer. The effect of wavelength of light on solar electrical performance. *In*: Proceedings of the ASME 2020 Power Conference collocated with the 2020 International Conference on Nuclear Engineering, Anaheim, California. 2020.
[41] PP Altermatt, Y Chen, Y Yang, A Ali and PJ Verlinden. Optical properties of industrially mass-produces crystalline silicon solar cells and prospects for improvements. *In*: Proceedings of the Optics for Solar Energy, Leipzig, Germany. 2016.
[42] JK Selj, D Young and S Grover. Optimization of the antireflection coating of thin epitaxial xrystalline silison solar cells. *Energ. Procedia* 2015; **77**, 248-52.
[43] MA Green and MJ Keevers. Optical properties of intrinsic silicon at 300K. *Progr. Photovoltaics Res. Appl*. 1995; **3**, 189-92.
[44] J Mullerova, P Sutta and M Hola. Optical absorption in Si:H thin film: Revisitting the role of the refractive index and the absorption coefficient. *Coatings* 2021; **11**, 1081.
[45] H Zhitao, C Jinkui, M Fantao and J Rencheng. Design and simulation of blue/violet sensitive photodetectors in silicon-on-insulator. *J. Semicond.* 2009; **30**, 104008.
[46] H Wang, X Liu and ZM Zhang. Absorption coefficients of crystalline silicon at wavelengths from 500 nm to 1,000 nm. *Int. J. Themphyics* 2013; **34**, 213-25.
[47] S Lorch. *Theory and measuring of antireflection coatings.* University of Ulm, Baden-Württemberg, Germany, 2003, p. 15-20.
[48] SB Khan, S Irfan, Z Zhuanghao and SL Lee. Influence of refractive index on antireflectance efficiency of thin films. *Materials* 2019; **12**, 1483.
[49] R Dewan, I Vasilev, V Jovanov and D Knipp. Optical enhancement and losses of pyramid textured thin-film silicon solar cells. *J. Appl. Phys*. 2011; **110**, 013101.
[50] T Lauinger, J Schmidt, AG Aberle and R Hezel. Record low surface recombination velocities on 1 V cm p-silicon using remote plasma silicon nitride passivation. *Appl. Phys. Lett*. 1996; **68**, 1232.
[51] R Hezel and K Jaeger. Low-temperature surface passivation of silicon for solar cells. *J. Electrochem. Soc.* 1989; **136**, 518.
[52] FL Riley. Silicon nitride and related materials. *J. Am. Ceram. Soc*. 2004; **83**, 245-65.
[53] P Hierrezuelo-Cardet, AF Palechor-Ocampo, J Caram, F Ventosinos, D Perez-del-Rey, HJ Bolink and JA Schmidt. External quantum efficientcy measurements used to study the stability of differently deposited perovskite solar cells. *J. Appl. Phys.* 2020; **127**, 235501.
[54] MM Hung, HV Han, CY Hong, KH Hong, TT Yang, P Yu, YR Wu, HY Yeh and HC Huang. Compound biomimetic structures for efficiency enhancement of $Ga_{0.5}In_{0.5}P$/GaAs/Ge triple junction solar cells. *Optic. Express* 2014; **22**, A295-300.
[55] MA Zahid, MQ Khokhar, Z Cui, H Park and J Yi. Improved optical and electrical properties for heterojunction solar cell using Al_2O_3/ITO double layer anti-reflective coating. *Results Phys.* 2021; **28**, 104640.
[56] T Markvart and L Castañer. *Chapter IA-1 - principles of solar cell operation*. *In*: A McEvoy, T Markvart and L Castañer (Eds.). Practical handbook of photovoltaics. 2nd ed. Academic Press, London, 2012.
[57] P Hersch and K Zweibel. Basic photovoltaic principles and methods. *Antimicrob. Agents Chemother.* 1982; **58**, 7250-7.
[58] T Tiedje, E Yablonovitch, GD Cody and BG Brooks. Limiting efficiency of silicon solar cells. *IEEE Trans. Electron. Dev*. 1984; **56**, 520-5.